

Figure S1. Expression of p21 and p27 at P8 in WT and *Rb* null retina
Real-time RT-PCR analysis of *Cdkn1a* (*p21*) and *Cdkn1b* (*p27*) genes in WT and *Rb* null retinas at P8. Error bar represent SD of measurements from three independent experiments.

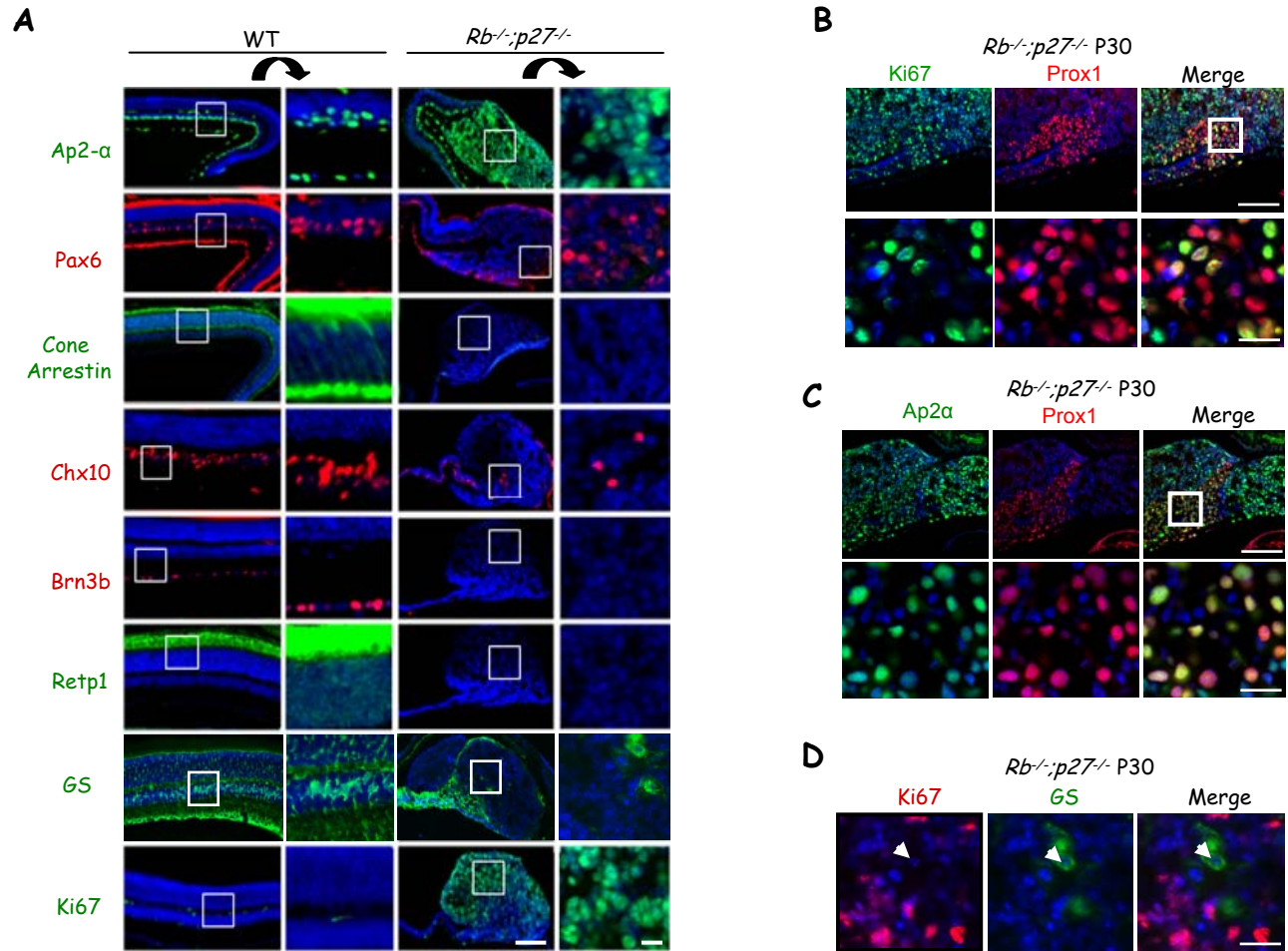


Figure S2. Emerging *Rb*^{-/-};*p27*^{-/-} tumors contain dividing cells positive for amacrine cell markers

(A) Marker analysis of P30 WT and *Rb*^{-/-};*p27*^{-/-} retina. Low magnification views are shown on the left (scale bar 100 μ m) and high magnification views of the boxed regions are shown on the right (scale bar 20 μ m). Emerging tumors stained primarily for Ap2 α (green), which specifically marks amacrine cells, Pax6 (red), which marks amacrine cells as well as other cell types, and Ki67 (green) which marks dividing cells. Tumors had no or very few cells that stained for markers of cone (Cone arrestin), bipolar (Chx10), ganglion (Brn3b) or rod (Retp1) cells. All sections in A were also stained with DAPI to mark nuclei (blue).

(B) Tumors at P30 were labeled with Ki67 (green) to mark dividing cells, Prox1 (red) which marks horizontal, bipolar and a subset of amacrine cells in normal adult retina, and DAPI to label nuclei (blue).

(C) Prox1⁺ cells (red) were amacrine-like as they co-stained for Ap2 α (green). Scale bar 100 μ m upper panel and 20 μ m lower panel.

(D) Tumors were stained for Ki67 and glutamine synthase (GS, green), which marks Müller glia. These cells, unlike those with amacrine markers were not dividing. Scale bar 20 μ m. In A-D, for simplicity "*Rb*^{-/-}" represents *α Cre*;*Rb*^{f/f}.

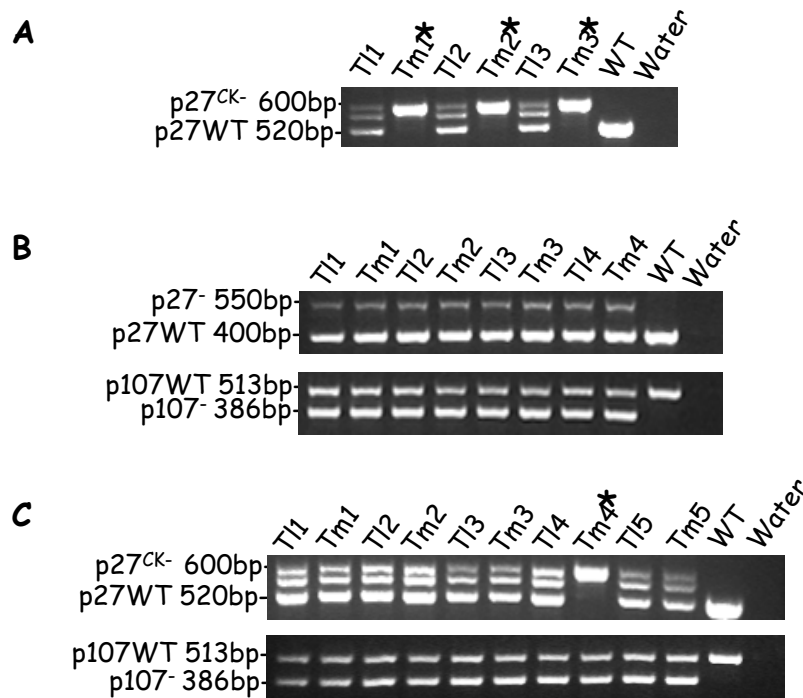


Figure S3. LOH analysis in heterozygotes

(A) Genotyping of tail (TI) and tumor (Tm) DNA for $p27^{CK-}$ allele in $\alpha Cre;Rb^{f/f};p27^{+/CK-}$ mice showing LOH as indicated by single 600 bp band for $p27^{CK-}$ knock-in allele and loss of 520 bp band for WT allele in tumor DNA for all three tumor samples. The $p27^{CK-}$ diagnostic primers also often generate a background band between the 600 bp and 520 bp fragments.

(B) Genotyping of four $\alpha Cre;Rb^{f/f};p107^{-/-};p27^{-/-}$ mice showing no LOH for $p27$ (upper panel; WT allele 400 bp and KO allele 550 bp) and $p107$ (lower panel; WT allele 386 bp and KO allele 513 bp).

(C) $\alpha Cre;Rb^{f/f};p107^{-/-};p27^{+/CK-}$ tumor showing LOH for $p27^{CK-}$ knockin allele in only a single tumor sample (Tm4; upper panel) and no LOH for $p107$ allele (lower panel).

* Tumor samples showing LOH.

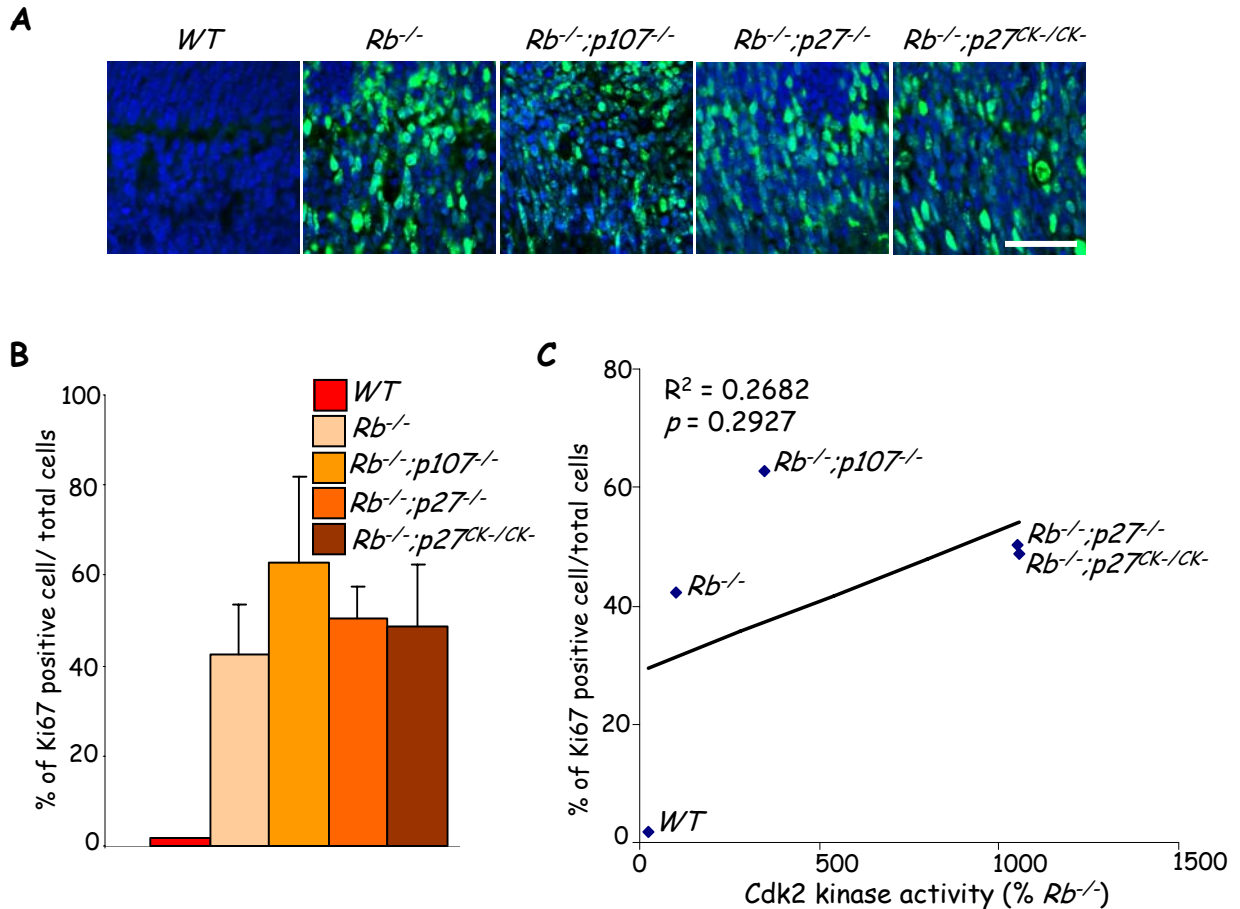


Figure S4. At P8 CDK2 activity does not correlate with cell cycle index (A) P8 retinas of the indicated genotypes were stained for Ki67 (green) and DAPI (blue). Scale bar 50 μ m. (B) Quantification Ki67 positive cells in indicated genotypes. Data are mean \pm SD. (C) Cdk2 kinase activity (percent of that in the *Rb* null retina) was plotted against percentage of Ki67⁺ cells at P8. *p* value was determined using a one-sample *t*-test for Pearson's product-moment correlational coefficient, *r*. All assays were carried out at least 3 times. For simplicity "*Rb*^{-/-}" represents α Cre;*Rbf*/*f*.

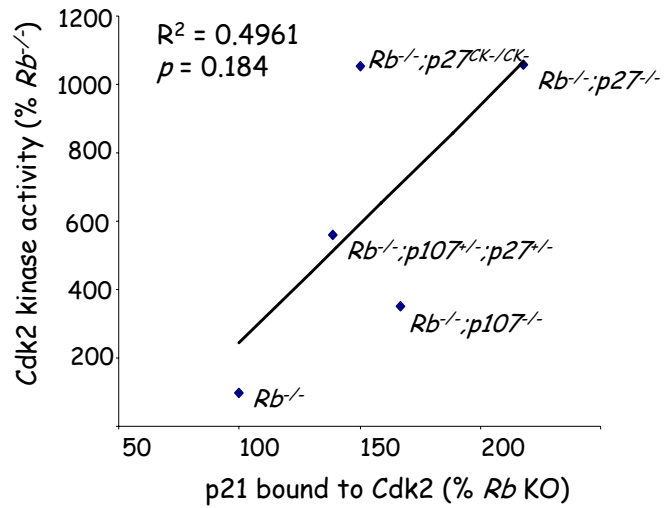


Figure S5. p21 levels bound to Cdk2 do not correlate with kinase activity
 Cdk2 kinase activity (from figure 3) was plotted against the amount of p21 bound to Cdk2. "*Rb*^{-/-}" is used to indicate *αCre;Rb^{f/f}*. *p* values were calculated using a one-sample *t*-test for Pearson's product-moment correlational coefficient, *r*.